iScience

CellPress
OPEN ACCESS

Article

Enterocyte superoxide dismutase 2 deletion drives obesity

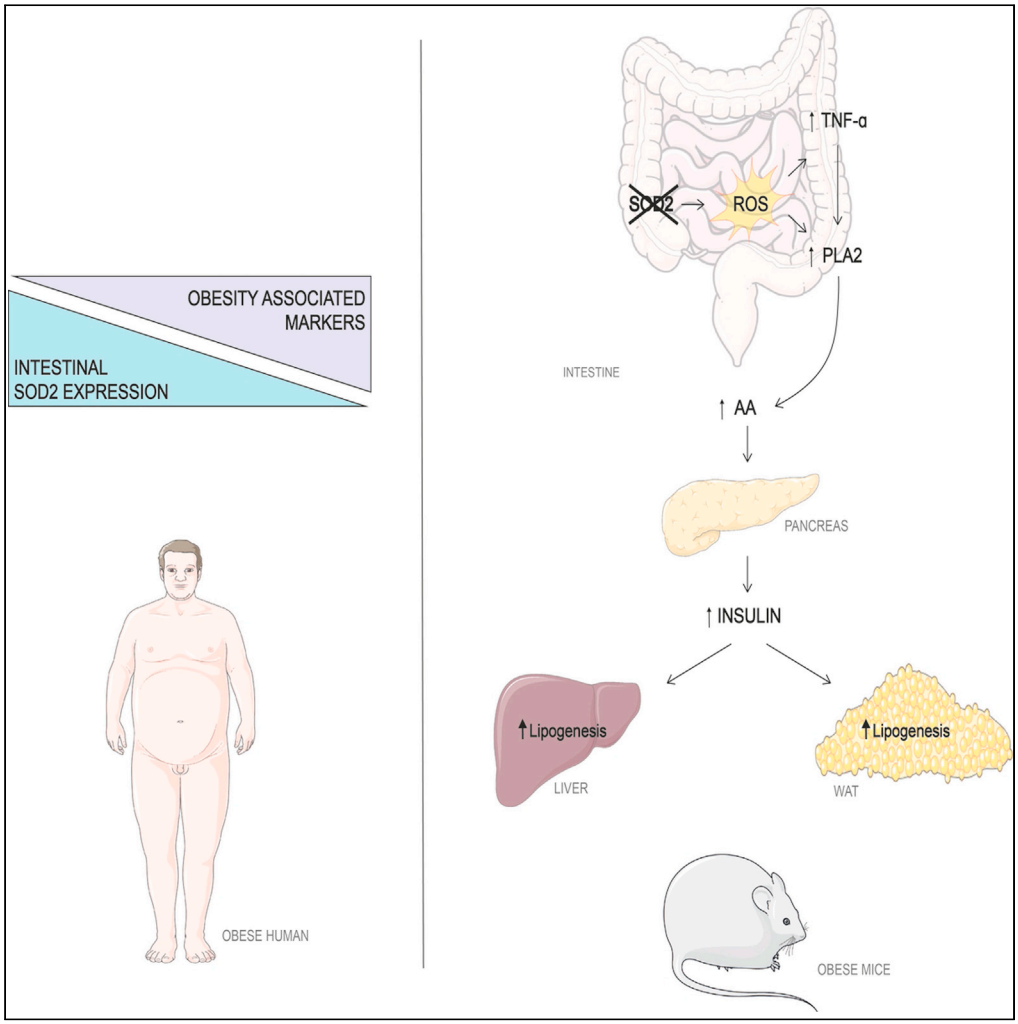

Oihane Garcia-Irigoyen, Fabiola Bovenga, Marilidia Piglionica, ..., Gaetano Villani, Massimo Federici, Antonio Moschetta

antonio.moschetta@uniba.it

Highlights

Intestinal deletion of SOD2 drives spontaneous obesity and inflammation in mice

SOD2 deficiency promotes phospholipase A2 activation and arachidonic acid release

SOD2 ablation in enterocytes generates a pro-lipogenic phenotype

Inverse relation between intestinal SOD2 and obesity features is present in humans

Garcia-Irigoyen et al., iScience *25*, 103707
January 21, 2022
https://doi.org/10.1016/j.isci.2021.103707

iScience

CellPress
OPEN ACCESS

Article

Enterocyte superoxide dismutase 2 deletion drives obesity

Oihane Garcia-Irigoyen,[1,12] Fabiola Bovenga,[1,12] Marilidia Piglionica,[1] Elena Piccinin,[1,2] Marica Cariello,[1] Maria Arconzo,[1] Claudia Peres,[1] Paola Antonia Corsetto,[3] Angela Maria Rizzo,[3] Marta Ballanti,[4] Rossella Menghini,[5] Geltrude Mingrone,[6,7,8] Philippe Lefebvre,[9] Bart Staels,[9] Takuji Shirasawa,[10] Carlo Sabbà,[1] Gaetano Villani,[2] Massimo Federici,[4,5,13] and Antonio Moschetta[1,11,13,14,*]

SUMMARY

Compelling evidence support an involvement of oxidative stress and intestinal inflammation as early events in the predisposition and development of obesity and its related comorbidities. Here, we show that deficiency of the major mitochondrial antioxidant enzyme superoxide dismutase 2 (SOD2) in the gastrointestinal tract drives spontaneous obesity. Intestinal epithelium-specific *Sod2* ablation in mice induced adiposity and inflammation via phospholipase A2 (PLA2) activation and increased release of omega-6 polyunsaturated fatty acid arachidonic acid. Remarkably, this obese phenotype was rescued when fed an essential fatty acid-deficient diet, which abrogates *de novo* biosynthesis of arachidonic acid. Data from clinical samples revealed that the negative correlation between intestinal *Sod2* mRNA levels and obesity features appears to be conserved between mice and humans. Collectively, our findings suggest a role of intestinal *Sod2* levels, PLA2 activity, and arachidonic acid in obesity presenting new potential targets of therapeutic interest in the context of this metabolic disorder.

INTRODUCTION

Oxidative stress has been long studied as a major cause of many diseases. Elevated levels of reactive oxygen species (ROS) have been linked to inflammation (Mittal et al., 2014), atherosclerosis (Halliwell, 1993), neurodegenerative diseases (Jenner, 1994), as well as obesity and its comorbidities (McMurray et al., 2016). However, the idea that ROS exclusively function as harmful molecules has been revised because sub-toxic levels of ROS can represent signaling pathways in a myriad of physiological mechanisms (Sies and Jones, 2020) and, in particular, in intestinal mucosal homeostasis (Bellafante et al., 2014; Campbell and Colgan, 2018; D'Errico et al., 2011), underlining the importance of tissue redox balance.

The intestinal tract serves as the first line of defence between the organism and its luminal environment and is continuously challenged by several insults. In order to preserve its tissue homeostasis, the intestinal epithelium has an enormous capacity for self-renewal. Every 3 to 5 days the intestinal mucosa is renewed via the proliferation, migration, and differentiation of the cells from the crypts to the apical compartment of the villus, where epithelial cells undergo apoptosis and are shed into the lumen (Lin and Barker, 2011). Redox signaling plays an essential role in the regulation of the self-renewal process of the gastrointestinal epithelium as ROS accumulation triggers apoptosis in the differentiated apical compartment (D'Errico et al., 2011). ROS are formed as natural by-products of the metabolism of oxygen being the mitochondrial respiratory chain, a major source in aerobic cells (Balaban et al., 2005; Murphy, 2009). Under physiological conditions, cells are protected against the oxidative stress by a set of oxygen radical scavengers, including superoxide dismutases.

Superoxide dismutases are a family of metal ion cofactor-requiring enzymes that function to precisely catalyze the dismutation of reactive superoxide anions into a more stable and readily diffusible H_2O_2 (Zelko et al., 2002). Among these, superoxide dismutase 2 (SOD2) is found exclusively within the mitochondria (Bresciani et al., 2015). The critical importance of this ROS scavenging enzyme was confirmed by the extremely short lifespan of homozygous SOD2 knockout mice which die within weeks from severe dilated cardiomyopathy and exhibit hypothermia, growth retardation, metabolic disruption, and lipid

[1]Clinica Medica "Cesare Frugoni", Department of Interdisciplinary Medicine, University of Bari "Aldo Moro", Piazza Giulio Cesare 11, 70124 Bari, Italy

[2]Department of Basic Medical Sciences, Neuroscience and Sense Organs, University of Bari "Aldo Moro", Piazza Giulio Cesare 11, 70124 Bari, Italy

[3]Department of Pharmacological and Biomolecular Sciences, University of Milan, Via D. Trentacoste 2, 20133 Milan, Italy

[4]Center for Atherosclerosis, Policlinico Tor Vergata, 00133 Rome, Italy

[5]Department of Systems Medicine, University of Rome Tor Vergata, 00133 Rome, Italy

[6]Department of Internal Medicine, Catholic University, Rome, Italy

[7]Fondazione Policlinico Universitario A. Gemelli IRCCS, Rome, Italy

[8]Diabetes and Nutritional Sciences, Hodgkin Building, Guy's Campus, King's College London, London, UK

[9]Université Lille, Inserm, CHU Lille, Institut Pasteur de Lille, U1011-EGID, F-59000 Lille, France

[10]Department of Molecular Gerontology, Tokyo Metropolitan Institute of Gerontology, 35-2 Sakae-cho, Itabashi-ku, Tokyo 173-0015, Japan

[11]IRCCS Istituto Tumori "Giovanni Paolo II", Viale O. Flacco 65, 70124 Bari, Italy

[12]These authors equally contributed

[13]Senior author

[14]Lead contact

Continued

accumulation in the liver (Li et al., 1995). Owing to these detrimental consequences, various tissue-specific SOD2 knockout mice have been designed using the Cre-loxp system (Shimizu et al., 2010) in order to elucidate the role of this enzyme in adult tissues. However, the importance of SOD2 in the gastrointestinal tract is still unknown.

Compelling evidence support an association between obesity and oxidative stress caused by excessive superoxide generation (Keaney et al., 2003). Indeed, a positive association has been described between obesity and Ala16Val *SOD2* gene polymorphism, which decreases the formation of the active SOD2 protein in the mitochondrial matrix (Montano et al., 2009). Obesity is associated with low-grade systemic inflammation and dysregulation of several organ systems, including adipose tissue, pancreas, liver, and gastrointestinal tract. Although the majority of the studies in obese humans and animal models have focused on adipose tissue as the source of pro-inflammatory cytokines, recent evidence support a role of intestinal inflammation as an early event in the pathogenesis of obesity (Ding and Lund, 2011). Thus, intestinal epithelium homeostasis imbalance due to a constant challenge by diet-derived oxidants as well as by endogenously generated ROS could be of crucial importance in the susceptibility to obesity and the development of obesity-related comorbidities, such as insulin resistance or type 2 diabetes. Consequently, in the present study, we focused on the function of the major mitochondrial antioxidant enzyme SOD2 in the intestine. Our data suggest that villin-driven intestinal SOD2 deletion drives spontaneous obesity through a mechanism involving enterocyte-specific phospholipase A2 (PLA2) activation and increased omega-6 polyunsaturated fatty acid arachidonic acid (AA).

RESULTS

Generation of intestine-specific SOD2 deficient mice

To study the role of mitochondrial SOD2 in the intestine, we generated mice harboring a specific ablation of *Sod2* gene for the intestinal epithelial tissue (iSOD2KO) by the Cre/loxp technique. To this end, mice overexpressing Cre-recombinase under the control of the Villin promoter were crossed with mice in which the third exon of the *Sod2* gene was flanked by loxp sequences in order to generate the iSOD2KO mice (Figure S1A). To confirm specific intestinal ablation of SOD2, we measured its mRNA content in the three regions of the small intestine, colon, liver and epididymal white adipose tissue (WAT) by quantitative real-time PCR. *Sod2* expression was extremely reduced in the intestinal tract of iSOD2KO mice compared to their SOD2flox littermates, while its expression was not significantly altered in non-intestinal tissues (Figure S1B).

Intestinal SOD2 deficiency drives obesity

In order to characterize the basal phenotype associated with intestinal SOD2 deficiency, iSOD2KO and SOD2flox mice were weighted monthly and sacrificed at the stage of 6 to 8 months old. A tendency toward increased nitrotyrosine (NITT) levels in iSOD2KO animals was detected when compared to control littermates. (Figure S1C). NITT is the by-product of the reaction of nitric oxide and superoxide. Its increase suggests that the ablation of SOD2 from the intestine is causing an increased oxidative damage to the enterocytes. The levels of malondialdehyde (MDA), an end product of lipid peroxidation, were also measured in the intestinal mucosa due to the important antioxidant activity of SOD2 enzyme. However, as previously described in SOD2 total body knockout (Li et al., 1995) and liver-specific SOD2-deficient mice (Ikegami et al., 2002), no differences in lipid peroxidation levels were seen between SOD2flox and iSOD2KO mice (Figure S1D). Notably, the assessment of *Nrf2* mRNA levels revealed an increased expression of this gene in iSOD2KO mice compared to controls, probably suggesting the existence of a compensatory mechanism to counteract the absence of SOD2 from the intestinal epithelium. Nevertheless, the expression of several antioxidant genes (Glutathione peroxidase 4, Thioredoxin 2, Peroxiredoxin 3, and NADPH Quinone Dehydrogenase 1) evaluated in all the intestinal tracts displayed no significant differences between the two genotypes (Figure S2).

Importantly, iSOD2KO mice showed a significant spontaneous increase in their body weight starting at 3 months of age and reached a body weight (41,71 $\pm$ 1,107 g) that was 22.2% higher as compared with SOD2flox littermates (34,13 $\pm$ 0,6391 g) at 8 months (Figure 1A). No differences in food intake were found between the two genotypes (Figure 1B). The higher body weight in iSOD2KO mice at the moment of the sacrifice (Figure 1C) was in accordance with the significantly elevated epididymal WAT weight (Figure 1D).

Obesity is associated with a chronic low-grade inflammation state (Ellulu et al., 2017). Correspondingly, histological analysis of haematoxylin-eosin staining showed inflammatory infiltrates in the liver and WAT, as

*Correspondence:
antonio.moschetta@uniba.it

https://doi.org/10.1016/j.isci.2021.103707

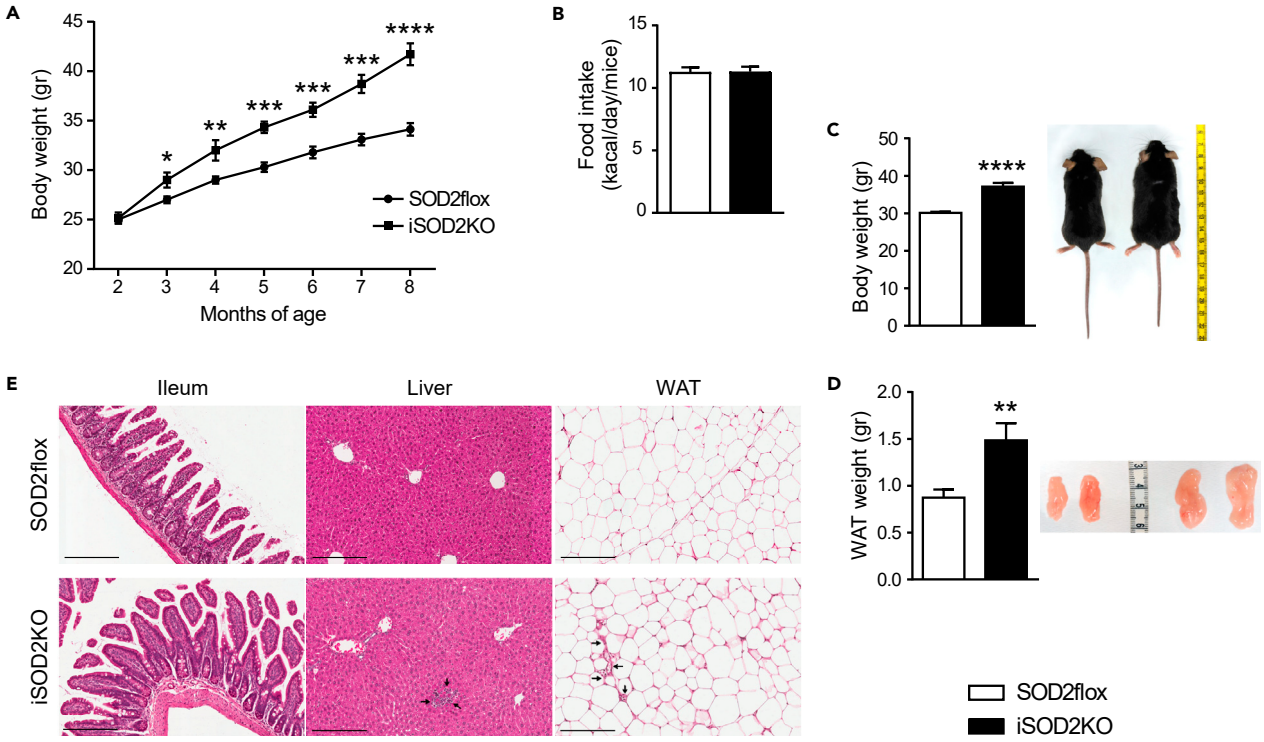
A
Body weight (gr)
Months of age
SOD2flox
iSOD2KO
B
Food intake (kcal/day/mice)
C
Body weight (gr)
D
WAT weight (gr)
E
Ileum
Liver
WAT
SOD2flox
iSOD2KO

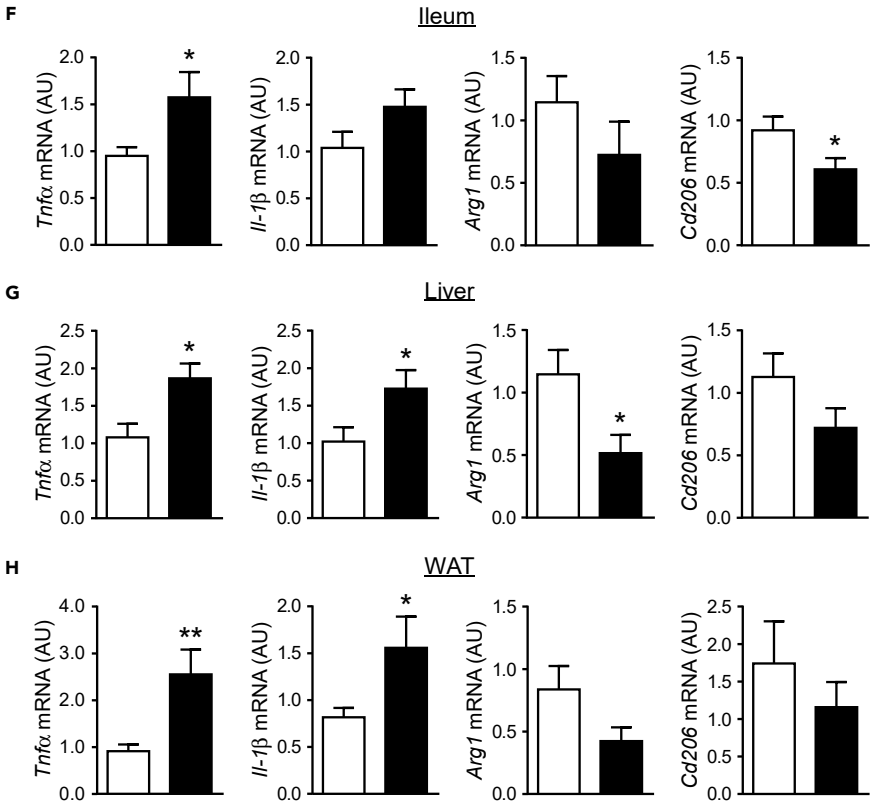
F
Ileum
G
Liver
H
WAT
Tnfα mRNA (AU)
Il-1β mRNA (AU)
Arg1 mRNA (AU)
Cd206 mRNA (AU)

Figure 1. Intestinal SOD2 deficiency induces overweight and pro-inflammatory phenotype in iSOD2KO mice

(A) Body weights measured monthly in SOD2flox and iSOD2KO mice under chow diet (*ad libitum*).

(B) Daily food intake in SOD2flox and iSOD2KO mice.

(C) Body and (D) WAT weights at 8 months of age in SOD2flox and iSOD2KO mice.

(E) Hematoxylin and eosin staining of ileum, liver, and WAT sections from SOD2flox and iSOD2KO mice (magnification 100X, scale bar: 200 μm). Arrows indicate the inflammatory infiltrates.

(F–H) Relative mRNA expression of inflammatory cytokines, *Tnfα* and *Il-1β*, and M2 macrophage markers, *Arg1* and *Cd206*, measured in the (F) ileum, (G) liver, and (H) WAT samples from SOD2flox and iSOD2KO by real-time qPCR using *Tbp* as a housekeeping gene. Comparison of flox and KO mice (n = 10) was performed using a Student *t* test. All data are represented as mean ± SEM. *$p<0.05$, **$p<0.01$, ***$p<0.001$, ****$p<0.0001$.

well as, a thickening of the muscularis layer and an increase of vascularization in the ileum of iSOD2KO animals (Figure 1E). However, no changes in the dimension and structure of villi and crypts were detected in iSOD2KO mice compared to controls (Figure S1E). Moreover, iSOD2KO mice did not display altered intestinal permeability, as indicated by the evaluation of the expression of genes encoding for tight junction proteins (Claudin-2, Zona Occludens-1, and Occludin) and the levels of lipopolysaccharides binding protein (LBP) (Figures S1F and S1G).

Pro-inflammatory and lipogenic phenotype in iSOD2KO mice

To further confirm the pro-inflammatory phenotype, we quantified the expression of a set of inflammatory cytokines and M1/M2 macrophage polarization markers (Tan et al., 2016). A clear tendency toward the pro-inflammatory M1 phenotype population was detected in the ileum, liver, and WAT of iSOD2KO mice as shown by the increased expression of *Tnfα* and *Il-1β* cytokine genes and the decreased expression of the M2 markers arginase 1 and CD206 (Figures 1F–1H). These results were confirmed in the entire intestinal tract, with the exception of the colon where the expression of the M2 markers were increased in iSOD2KO mice compared to control littermates (Figure S3). Altogether, these data suggest that the absence of SOD2 in the gut is not only generating a localized inflammatory response in the intestinal tract but also a remote pro-inflammatory condition on liver and adipose tissue.

Following this, the expression of a number of lipogenic enzymes was analyzed to further explain the increased body and WAT weight observed in iSOD2KO mice. These animals, under basal conditions (chow diet), displayed higher expression of genes involved in lipid synthesis and its regulation, including *Srebp1c*, *Fasn*, and *Acc*, especially in liver and WAT (Figures 2A–2C). In accordance with the increased lipogenesis, the levels of triglycerides, cholesterol, and phospholipids measured in the plasma of iSOD2KO mice were significantly higher than those detected in SOD2flox littermates (Figure 2D). Thus, the deletion of SOD2 in the intestinal tract promotes a pro-lipogenic phenotype in iSOD2KO mice that leads to an increased body weight.

SOD2 ablation in enterocytes significantly increases circulating insulin and glucose levels

Among the overexpressed lipogenic genes in iSOD2KO mice, we observed a major fold change in the expression of *Srebp1c* (Figures 2A–2C). *Srebp1c* mRNA has been described to be robustly elevated by insulin in mouse and rat livers (Owen et al., 2012). The strong association of obesity with type 2 diabetes and insulin resistance has been recognized for decades. In this context, we measured fasting glucose and insulin plasma levels of 6- to 8- months-old iSOD2KO and SOD2flox mice and the HOMA-IR (Homeostatic Model Assessment for Insulin Resistance) was then calculated. Intestinal SOD2 ablation significantly increased circulating insulin levels (Figure 3A) and HOMA-IR (Figure 3B) in iSOD2KO animals. Moreover, these mice display a tendency to increase in the plasma level of Glucagone-Like Peptide 1 (GLP-1) (Figure 3C). Fasting blood glucose levels were also significantly higher in iSOD2KO mice. These mice also displayed difficulties in the clearance of orally administered glucose as demonstrated by the higher glucose curve during oral glucose tolerance test (OGTT) (Figure 3D). The pancreatic histological samples (Figure 3E) showed larger Langerhans islets in iSOD2KO pancreas in contrast to the ones observed in SOD2flox mice, even in fasting state. The data were confirmed by measuring the area of the insulin immunostaining, which showed a significantly higher average area of the Langerhans islets in the pancreas of iSOD2KO mice (Figure 3F). Based on these observations, we can conclude that the absence of intestinal SOD2 stimulates insulin production and, therefore, induces a lipogenic response in the liver and WAT that promotes obesity.

Increased intestinal PLA2 activity in iSOD2KO mice: intestinal AA as the cause of obesity?

In the context of the pro-inflammatory state observed both locally in the SOD2-deficient intestine, as well as in liver and WAT of the iSOD2KO mice, the increase in *Tnfα* could play a role, due to its crosstalk with

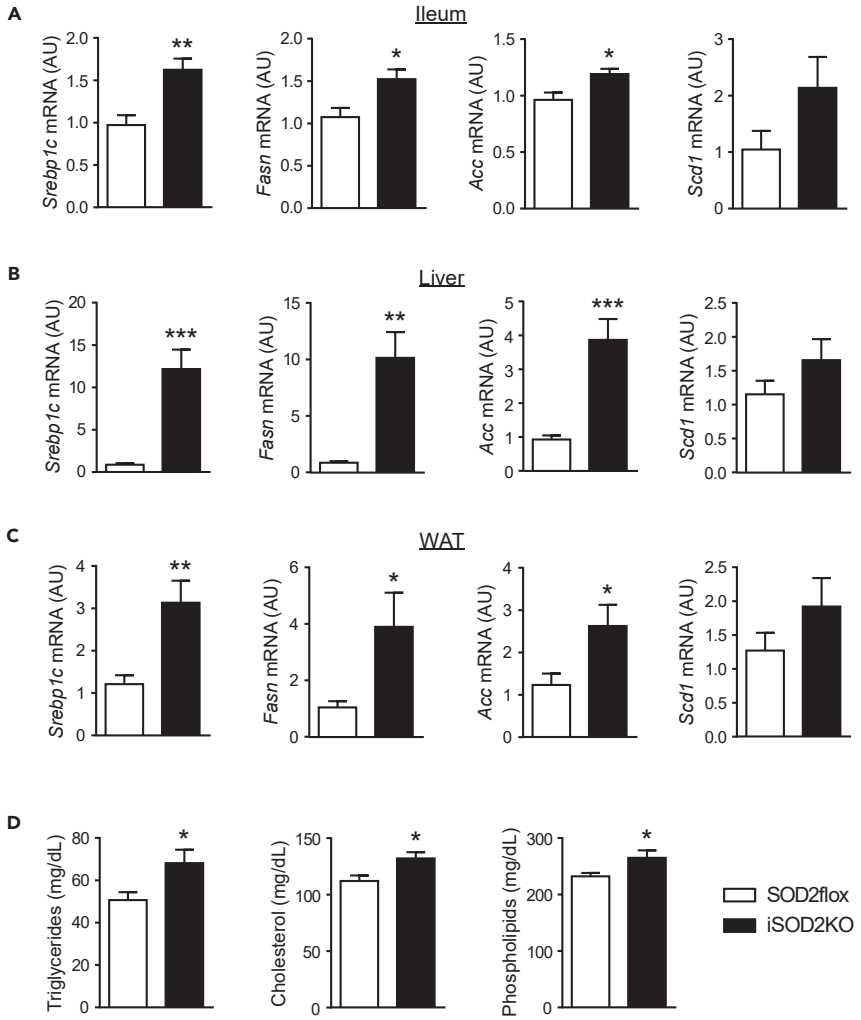

Figure 2. Increased lipogenesis in iSOD2KO mice

Relative mRNA expression of genes involved in lipogenesis measured in (A) ileum, (B) liver, and (C) WAT from SOD2flox and iSOD2KO mice by real-time qPCR using *Tbp* as a housekeeping gene.

(D) Plasma triglycerides, cholesterol, and phospholipids levels were measured in SOD2flox and iSOD2KO mice at 8 months of age. Comparison of flox and KO mice (n = 10) was performed using a Student *t* test. All data are represented as mean ± SEM. **p*<0.05, **p<0.01, ****p*<0.001.

ROS (Blaser et al., 2016). In particular, an increase in arachidonic acid (AA) is often associated with higher levels of TNFα as an effect of a TNFα-dependent activation of the cytosolic phospholipase A2 (cPLA2) (Hayakawa et al., 1993; Heller and Kronke, 1994; Hoeck et al., 1993). Furthermore, the mitochondrial PLA2 activity can be also activated by superoxide anion (Madesh and Balasubramanian, 1997). PLA2 catalyses the hydrolysis of the sn-2 ester bond of membrane phospholipids to liberate preferentially AA and lysophospholipids (Murakami and Kudo, 2002). AA has been shown to be positively associated with obesity (Naughton et al., 2016; Pickens et al., 2017) and insulin secretion from the islets of Langerhans (Band et al., 1993; Persaud et al., 2007), making this polyunsaturated omega-6 fatty acid a possible candidate to explain the metabolic alterations observed in iSOD2KO mice.

Consequently, we measured PLA2 activity and we show here that the absence of SOD2 in the intestinal epithelial cells increased PLA2 activity in the ileum mucosa samples of iSOD2KO mice (Figure 4A) along with the release of AA (Figure 4B). Simultaneously, the long-chain polyunsaturated (LCPUFA) omega-6/omega-3 free fatty acid ratio, represented as AA/eicosapentaenoic acid (EPA)+docosahexaenoic acid (DHA), was significantly higher in the plasma of iSOD2KO mice (Figure 4C).

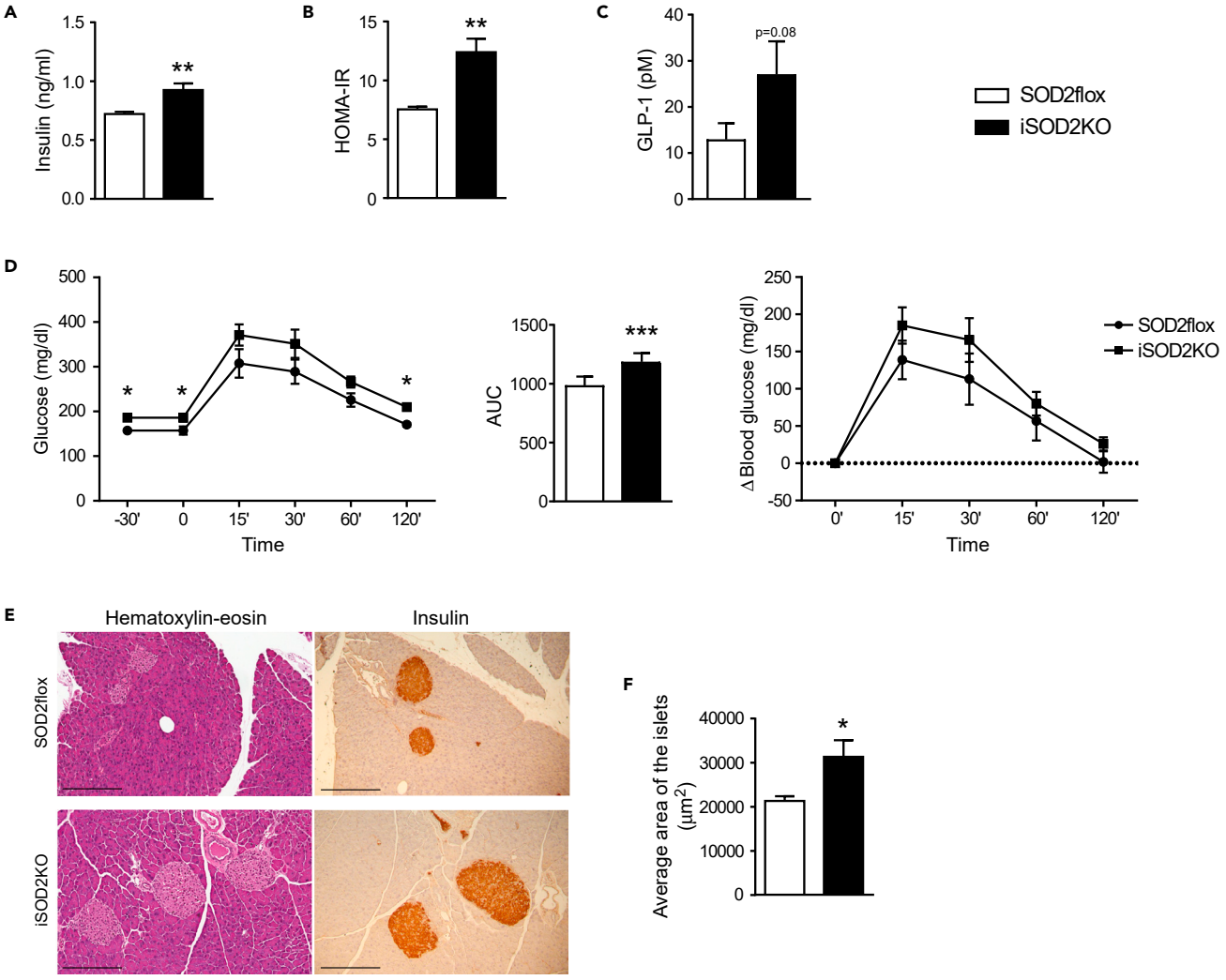

Figure 3. SOD2 ablation in intestinal tract increases pancreatic insulin secretion and HOMA-IR

(A) Plasma insulin levels were measured after an overnight fasting in SOD2flox and iSOD2KO mice.

(B) Fasting insulin and glucose (from OGTT) values were used to calculate HOMA-IR in order to assess insulin resistance [(fasting glucose mmol/L x fasting insulin mU/L)/22,5)].

(C) Plasma GLP-1 level in SOD2flox and iSOD2KO mice.

(D) SOD2flox and iSOD2KO mice were subjected to an OGTT: after overnight fasting blood glucose was measured, 2mg/kg glucose was administered via gavage and blood glucose was measured 15, 30, 60, and 120 min afterward. AUC curve was calculated.

(E) Hematoxylin and eosin staining and insulin immunostaining of pancreas tissue sections from SOD2flox and iSOD2KO mice (magnification 100X, scale bar: 200 μm).

(F) The average area of the Langerhans islets was determined by measuring the insulin-inmunostained area in 6 different 10X microscopic fields from 5 mice per group. Comparison of flox and KO mice (n = 5–10) was performed using a Student *t* test. All data are represented as mean ± SEM. *$p<0.05$, **$p<0.01$, ***$<p<0.001$

Essential fatty acid-deficient diet prevents obesity and impaired insulin secretion in iSOD2KO mice

Because ablation of SOD2 in the intestine drove susceptibility to obesity and hyperinsulinemia and we hypothesized that this event would be driven by higher circulating levels of AA due to increased enterocyte PLA2 activity, we next explored whether this condition could be reverted by a reduction of AA production. To this end, we administered an essential fatty acid-deficient (EFAD) diet to 3 months old SOD2flox and iSOD2KO mice for a period of 3 months. The absence of essential fatty acids in the diet effectively stopped *de novo* biosynthesis of AA, thus reducing AA release from membrane phospholipids and, consequently,

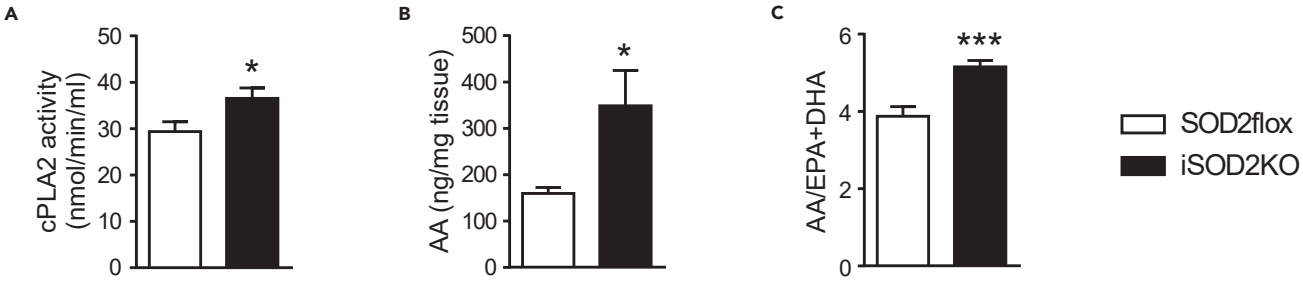

Figure 4. SOD2 deletion promotes intestinal PLA2 activation and AA release

(A) cPLA2 activity and (B) free AA levels were measured in ileum mucosa samples from SOD2flox and iSOD2KO mice.

(C) Plasma-free AA, EPA, and DHA levels were measured and omega-6/omega-3 (AA/EPA + DHA) ratio was calculated. Comparison of flox and KO mice (n = 6–10) was performed using a Student t test. All data are represented as mean ± SEM. *p<0.05, ***p<0.001.

circulating free AA levels (Figure S4). Within one month of EFAD feeding, the body weight difference between iSOD2KO and control mice completely disappeared (Figure 5A) with food intake being comparable in the two strains (Figure 5B). Interestingly, after 3 months under EFAD diet the body and WAT weights did not differ between the two mouse groups (Figures 5C and 5D). Furthermore, histological analysis of hematoxylin-eosin staining showed a slightly exacerbated inflammation in the ileum of iSOD2KO animals (Figure 5E), accompanied by an increased expression of the pro-inflammatory cytokine *Il-1β* (Figure S5A). On the contrary, no significant differences were shown in the inflammatory state of the liver and WAT between SOD2flox and iSOD2KO animals (Figures 5E and S5B and S5C).

The increased lipogenesis observed in the ileum, liver, and WAT in iSOD2KO mice under regular chow diet (Figures 2A–2C) was reverted by EFAD diet, as well as the levels of triglycerides, cholesterol, and phospholipids measured in the plasma of these animals (Figures 6A–6D). The increased plasma LC-PUFA omega-6/omega-3 ratio (AA/EPA + DHA) ratio observed in chow diet fed iSOD2KO mice did also disappear (Figure 6E). Consequently, fasting glucose and insulin levels, along with the HOMA-IR, were normalized after 3 months of EFAD diet (Figures 6F–6H). Accordingly, the area of the insulin-producing pancreatic islets did not differ between the iSOD2KO and SOD2flox littermates under the EFAD diet (Figures 6I and 6J).

Taken together, these results strongly suggest that intestinal-specific SOD2 deletion drives obesity by the increase of AA due to activation of PLA2 in the enterocytes.

Association of obesity features with intestinal SOD2 levels in humans

To understand whether our findings are reproducible also in humans, we analyzed the FLOROMIDIA database (Kappel et al., 2020) which allows to explore correlations between colon transcriptomics and clinical and metabolomics data in human subjects with different degrees of body mass index (BMI). Our purposing analysis revealed that low SOD2 levels in the intestine of these patients were associated with elevations in obesity-associated markers including BMI, waist circumference, and plasma omega-6/omega-3 fatty acid ratio. This negative correlation with SOD2 was found to be significative for BMI and AA/EPA + DHA ratio (Figure 7). We found that 2-h OGTT blood glucose levels and the OGTT area under the curve (AUC) have a trend to anti-correlate to SOD2 expression although not significantly when analyzed with Spearman correlation (Figure 7). The inverse relationship between intestinal SOD2 levels and obesity features in human patients is in accordance with the phenotype observed in our iSOD2KO mice, further confirming the hypothesis that mitochondrial antioxidant enzyme SOD2 in the intestinal tract is implicated in the susceptibility to obesity.

DISCUSSION

Mounting evidence support an involvement of oxidative stress (Higdon and Frei, 2003) and intestinal inflammation as early events that precedes and predisposes to obesity and insulin resistance (Ding and Lund, 2011; Spagnuolo et al., 2010). Mitochondria play an essential role in maintaining intestinal epithelium redox homeostasis being at the same time as the main source as well as the primary target of intracellular ROS. SOD2, a ROS-scavenging enzyme that catalyses the dismutation of reactive superoxide anions to H_2O_2, is found exclusively within the mitochondria. The critical cytoprotective action of this enzyme has

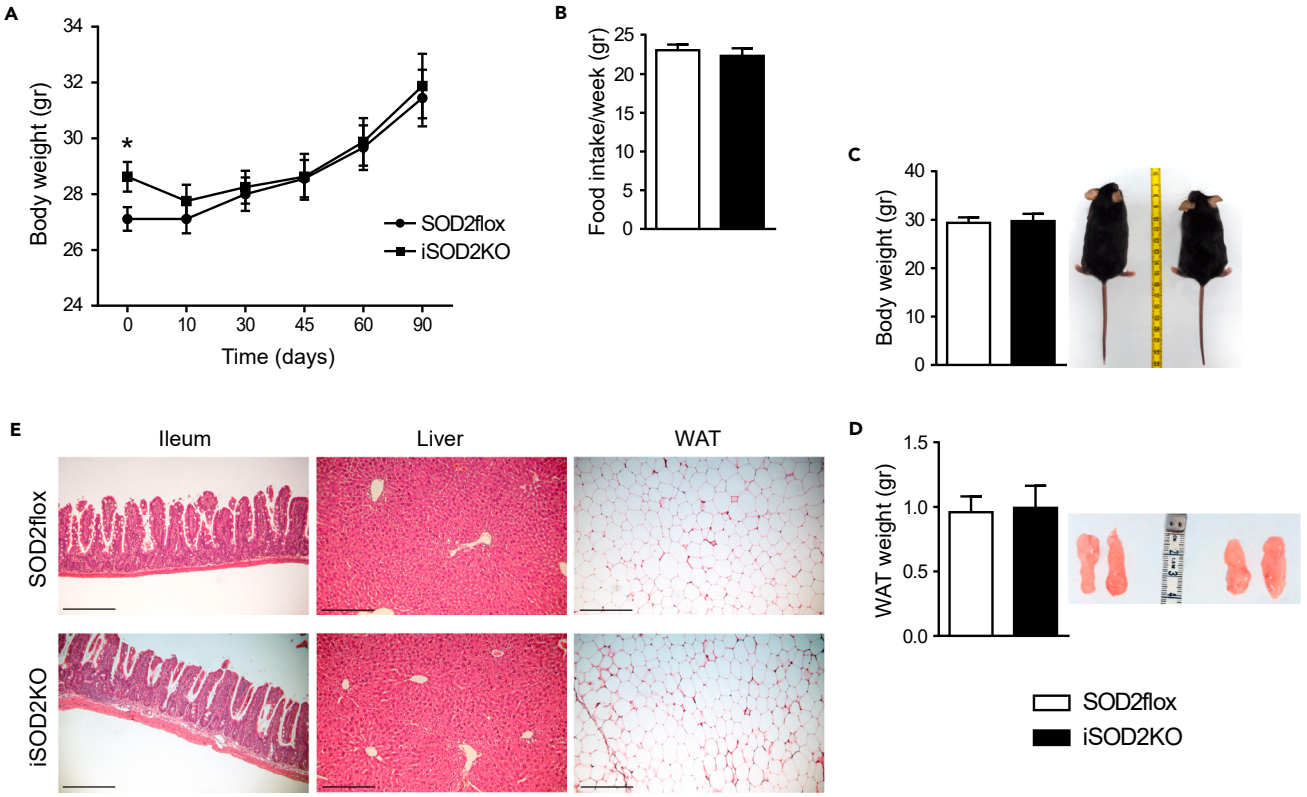

Figure 5. EFAD diet prevents overweight in iSOD2KO mice

(A) Body weight change during 3 months EFAD diet feeding in SOD2flox and iSOD2KO mice.

(B) Weekly food intake in SOD2flox and iSOD2KO mice.

(C) Body and (D) WAT weights in SOD2flox and iSOD2KO mice after 3 months under EFAD diet.

(E) Hematoxylin and eosin staining of ileum, liver, and WAT sections from EFAD-fed SOD2flox and iSOD2KO mice (magnification 100X, scale bar: 200 μm).

Comparison of flox and KO mice (n = 7–8) was performed using a Student t test. All data are represented as mean ± SEM. *$p<0.05$.

been confirmed by the extremely short lifespan of total body SOD2 knockout mice, which die within weeks after birth (Li et al., 1995). Thus, to study the implication of gastrointestinal SOD2 deficiency and its potential link to obesity, we generated mice carrying a specific deletion of the third exon of the *Sod2* gene in villin-expressing intestinal epithelial cells.

We observed that iSOD2KO mice were overweight compared to their counterparts beginning at 3 months of age and had significantly larger epididymal adipose fat pads. The body weight difference increased to a greater extent during aging, even though no differences in food intake (regular chow diet) were found. In accordance with the increased adiposity, iSOD2KO mice displayed higher expression of genes involved in intestine, liver, and WAT lipogenesis. As a consequence, the levels of triglycerides, cholesterol, and phospholipids measured in the plasma of iSOD2KO mice were significantly higher than those detected in SOD2-flox littermates.

Because obesity is associated with a chronic low-grade inflammation (Ellulu et al., 2017) and superoxide anions have pro-inflammatory roles (Alzoghaibi, 2013), a potential therapeutic role of SOD2 in inflammatory disorders has been proposed (Dowling et al., 1993; Li and Zhou, 2011). In the present study, we show a clear pro-inflammatory phenotype in small intestine, liver, and WAT of iSOD2KO mice accompanied by high expression levels of *Tnf-α* and *Il-1β* and by a clear tendency toward the pro-inflammatory M1 macrophage polarization. Remarkably, the phenotype of the iSOD2KO mice is unique among previously described tissue-specific SOD2-deficient mice (Shimizu et al., 2010). Although total body SOD2 knockout mice showed accumulation of lipid in liver, the liver-specific SOD2-deficient mice did not present gross histological abnormalities or biochemical defects (Ikegami et al., 2002). In addition, heart/muscle-specific SOD2-deficient mice showed growth retardation and a 25% reduction in body weight compared with

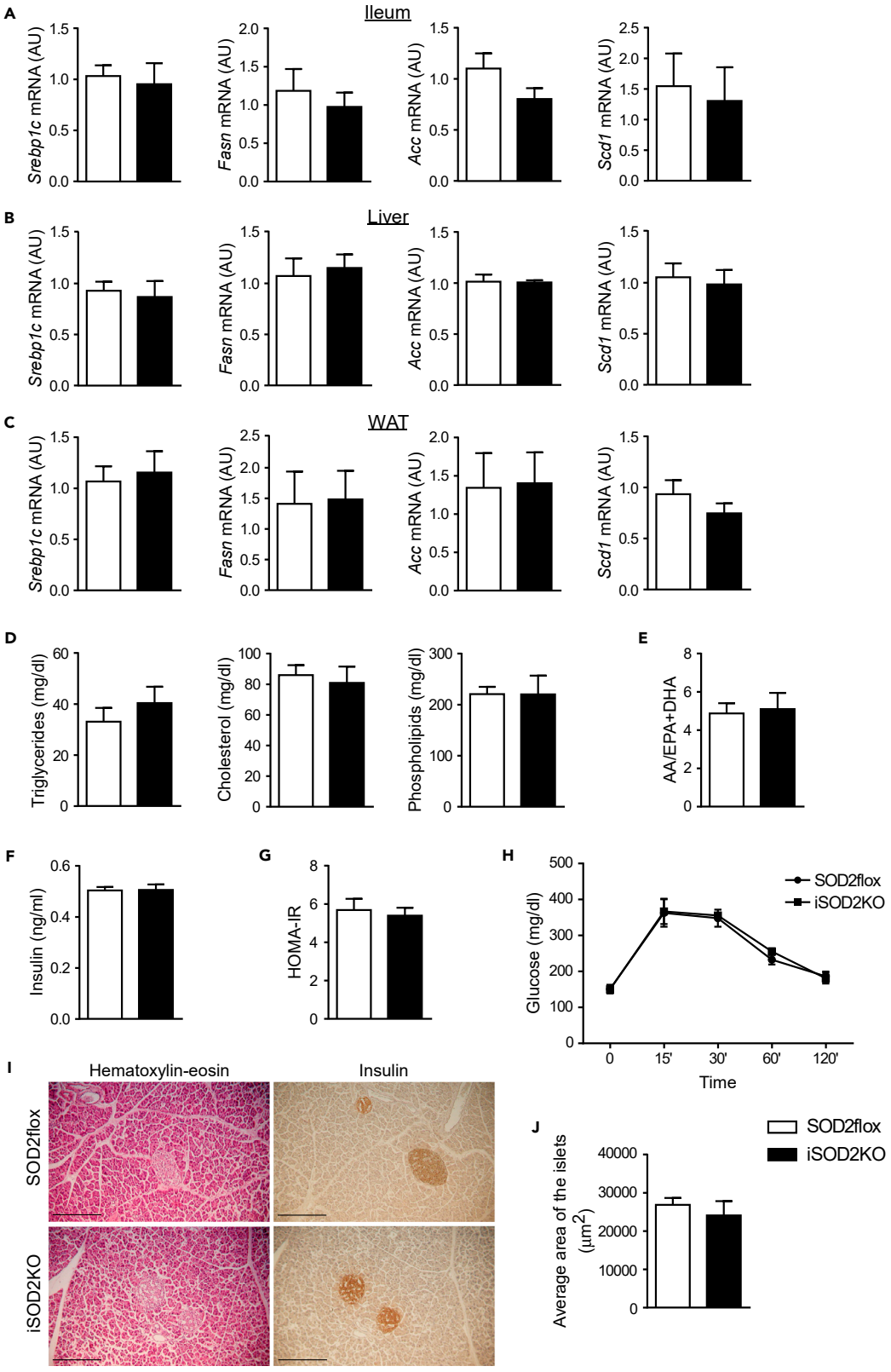
A
Ileum
Srebp1c mRNA (AU)
Fasn mRNA (AU)
Acc mRNA (AU)
Scd1 mRNA (AU)
B
Liver
C
WAT
D
Triglycerides (mg/dl)
Cholesterol (mg/dl)
Phospholipids (mg/dl)
E
AA/EPA+DHA
F
Insulin (ng/ml)
G
HOMA-IR
H
Glucose (mg/dl)
SOD2flox
iSOD2KO
0
15'
30'
60'
120'
Time
I
Hematoxylin-eosin
Insulin
SOD2flox
iSOD2KO
J
Average area of the islets (μm2)
SOD2flox
iSOD2KO

Figure 6. EFAD diet normalizes impaired lipogenesis and insulin secretion in iSOD2KO mice

Relative mRNA expression of genes involved in lipogenesis measured in (A) ileum, (B) liver, and (C) WAT from EFAD diet-fed SOD2flox and iSOD2KO mice by real-time qPCR using Tbp as a housekeeping gene. Plasma (D) triglycerides, cholesterol, phospholipids, and (E) free AA, EPA, and DHA levels were measured in SOD2flox and iSOD2KO after 3 months under EFAD diet, (E) omega-6/omega-3 (AA/EPA + DHA) ratio was then calculated. (F) Plasma insulin levels were measured after an overnight fasting in EFAD diet-fed SOD2flox and iSOD2KO mice.

(G) Fasting insulin and glucose (from OGTT) values were used to calculate HOMA-IR in order to assess insulin resistance [(fasting glucose mmol/L x fasting insulin mU/L)/22,5)].

(H) EFAD-fed SOD2flox and iSOD2KO mice were subjected to an OGTT: after overnight fasting blood glucose was measured, 2mg/kg glucose was administered via gavage and blood glucose was measured 15, 30, 60, and 120 min afterward.

(I) Hematoxylin and eosin staining and insulin immunostaining of pancreas tissue sections from fasted SOD2flox and iSOD2KO mice fed with EFAD diet for 3 months (magnification 100X, scale bar: 200 μm). (E) The average area of the Langerhans islets was determined by measuring the insulin-inmunostained area in 6 different 10X microscopic fields from 5 mice per group. Comparison of flox and KO mice (n = 5–8) was performed using a Student *t* test. All data are represented as mean ± SEM.

control mice (Nojiri et al., 2006) and adipocyte-specific SOD2-deficient model exhibited protection from diet-induced obesity (Han et al., 2016).

Insulin resistance and type 2 diabetes are well known obesity-related comorbidities. Nevertheless, whether it is the enlarged adipose tissue mass the cause of systemic insulin resistance or, inversely, insulin resistance and hyperinsulinemia, the contributors of the development of obesity are not completely defined (Kahn and Flier, 2000). iSOD2KO mice present increased fasting glucose and insulin levels and an elevated HOMA-IR that are suggestive of an insulin resistance condition. SREBP1C is robustly elevated by insulin in mouse and rat livers (Owen et al., 2012), suggesting that the elevated insulin levels found in the plasma of iSOD2KO mice could have fostered the lipogenic response observed in the liver of these animals.

Furthermore, iSOD2KO mice also show an increase in AA due to the activation of PLA2 by TNFα (Hayakawa et al., 1993; Heller and Kronke, 1994; Hoeck et al., 1993) as well as by superoxide anions (Madesh and Balasubramanian, 1997). This could represent a possible mechanism for a systemic impact of the local inflammation caused by the SOD2 deficiency-dependent alteration of intestinal redox homeostasis. Moreover, AA has been shown to be positively associated with insulin secretion from the beta cells of the pancreatic islets (Band et al., 1993; Persaud et al., 2007), which is in accordance with the larger Langerhans islets observed in the pancreas of iSOD2KO mice and the increased fasting insulin levels measured in their plasma.

The increased release of AA also elevates the bioactive long-chain polyunsaturated (LC-PUFA) omega-6/omega-3 ratio (AA/EPA + DHA) in the plasma of iSOD2KO mice, indicating a possible involvement of pro-inflammatory (omega-6) lipid mediators in this process. The effect of the diet in the risk for obesity is indisputable. The increased omega-6 fatty acid and decreased omega-3 fatty acid intake in the so called Western diet has resulted in an unhealthily elevated omega-6/omega-3 ratio (Simopoulos, 2016). Omega-3 and omega-6 polyunsaturated fatty acids play divergent roles in adipogenesis (Gaillard et al., 1989), lipid homeostasis (Jump et al., 1994), and systemic inflammation (James et al., 2000), eliciting different effects on body weight gain. Notably, omega-6 fatty acid-derived eicosanoid metabolites, such as prostaglandin E2 synthesized from AA, are more potent mediators of inflammation than those derived from omega-3 fatty acids (Simopoulos, 2016). AA cascade, for instance, is a well-recognized mediator of adipose inflammation (Miyamoto et al., 2019). In addition, several experimental and prospective studies have shown that a high omega-6/omega-3 ratio contributes to the prevalence of atherosclerosis (Kromhout and de, 2014), diabetes, and obesity (Donahue et al., 2011; Wang et al., 2016).

Remarkably, when fed an EFAD diet, the lack of intestinal SOD2-induced obese phenotype in mice was rescued. Essential omega-3 and omega-6 polyunsaturated fatty acids, alpha linolenic acid (ALA) and linoleic acid (LA), respectively, cannot be produced by humans, and other mammals including mice, thereby they must be obtained through the diet. Both essential fatty acids are metabolized to longer-chain fatty acids, such as AA from LA, and EPA and DHA from ALA (Simopoulos, 2016). Reducing *de novo* synthesis and, hence, the release of AA by the administration of the EFAD diet, we managed to normalize the body and WAT weights, insulin and glucose levels, HOMA-IR, and plasma omega-6/omega-3 LC-PUFA ratio, triglyceride, cholesterol, and phospholipid levels in iSOD2KO mice.

In conclusion, the overweight insulin resistant phenotype of iSOD2KO mice supports the idea that an altered redox signaling in the gastrointestinal tract could be crucial in the susceptibility to metabolic

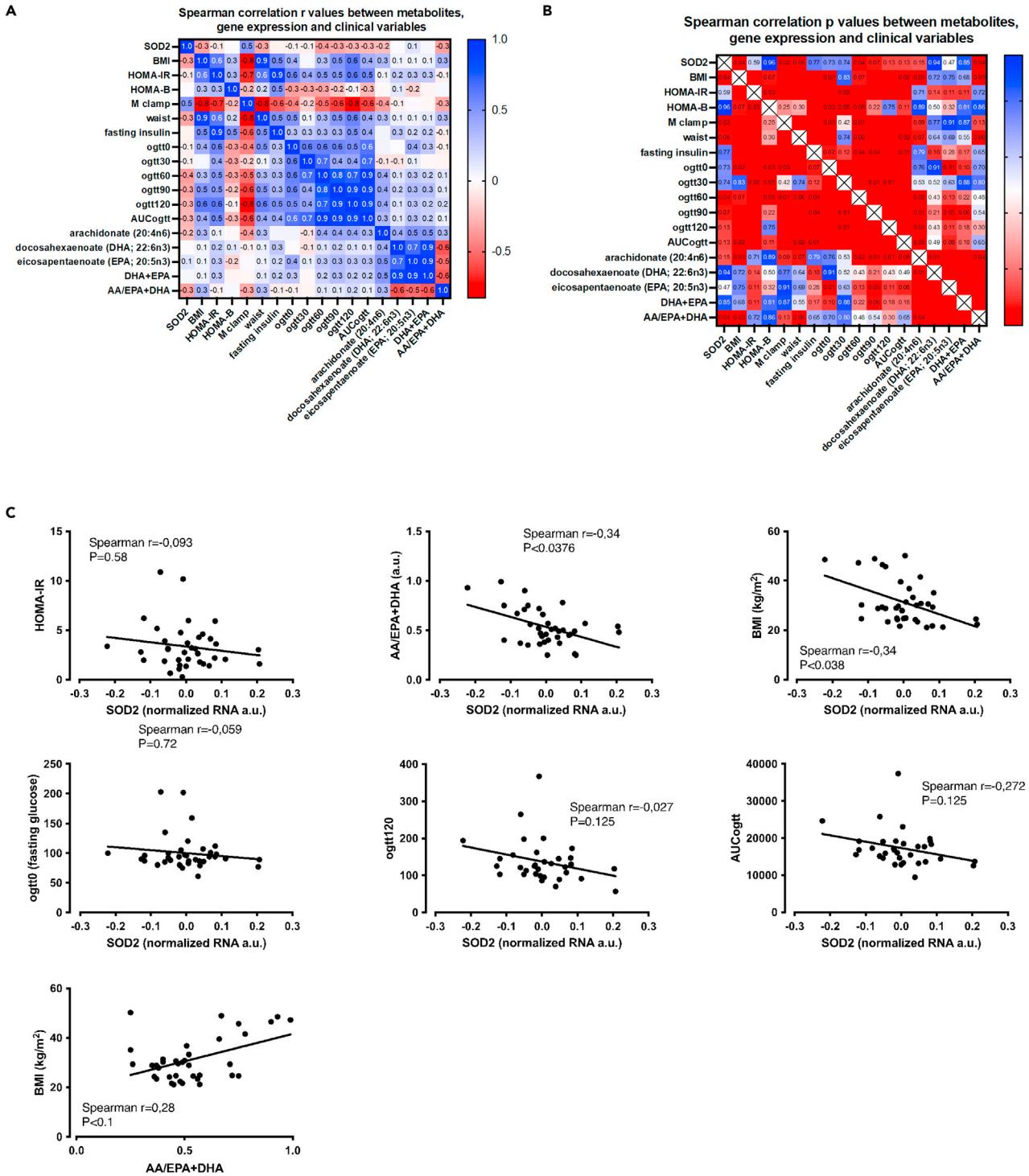

Figure 7. Intestinal SOD2 levels are associated with obesity features in human subjects

Spearman correlation analysis of SOD2 with HOMA-IR, AA/EPA + DHA, BMI, OGTT 0 min, OGTT 120 min, and OGTT AUC (A). Heatmaps of Spearman correlation r values (B) and p values (C) between metabolites and clinical variables.

disorders. This negative relationship between intestinal SOD2 levels and obesity features appears to be conserved between mice and humans as, according to our data, low SOD2 levels in the intestine of the FLOROMIDIA database human subjects correlated with increased BMI and AA/EPA + DHA ratio. Obesity

is a worldwide epidemic and the understanding of its molecular roots is essential in order to improve the prevention and treatment of this condition. In this context, the findings of the present study support a role of intestinal SOD2 levels, PLA2 activity, and AA in obesity presenting new potential targets in the treatment of this metabolic disorder.

Limitation of the study

There are some limitations of this study. First, our data demonstrated that intestinal SOD2 deletion is associated with increased ROS by-products and subsequent protein damage. However, we did not measure hydrogen peroxide (H_2O_2) formation because it is challenging to perform *in vivo* on intestinal mucosa. Second, although we described iSOD2KO animals as hyperinsulinemic via glucose tolerance test and HOMA-IR, we did not perform the gold standard euglycemic clamp to assess insulin resistance.

STAR★METHODS

Detailed methods are provided in the online version of this paper and include the following:

- KEY RESOURCES TABLE
- RESOURCE AVAILABILITY
  - Lead contact
  - Materials availability
  - Data and code availability
- EXPERIMENTAL MODEL AND SUBJECT DETAILS
  - Generation of mouse models and experimental settings
  - Human samples
- METHOD DETAILS
  - RNA extraction and real time qPCR
  - Histological and immunohistochemical studies
  - Plasma analysis
  - Oral glucose tolerance test
  - HOMA-IR
  - Lipid peroxidation
  - PLA2 activity
  - Lipid extraction
  - Free fatty acid analysis
- QUANTIFICATION AND STATISTICAL ANALYSIS

SUPPLEMENTAL INFORMATION

Supplemental information can be found online at https://doi.org/10.1016/j.isci.2021.103707.

ACKNOWLEDGMENTS

A. Moschetta is funded by: Interreg V-A Greece-Italy 2014-2020- SILVER WELLBEING, MIS5003627; MIUR-PRIN 2017 n.2017J3E2W2; EU-JPI HDL-INTIMIC–MIUR FATMAL; MIUR-PON "R&I" 2014-2020 "BIOMIS" cod.ARS01_01220; POR Puglia FESR–FSE2014-2020,"INNOMA"cod. 4TCJLV4. E. Piccinin is funded by PON-AIM 1853334 - Attività 2, linea 1. The authors acknowledge Smart Servier Medical Art (http://smart.servier.com/) for providing comprehensive medical and biological figures for the graphical abstract.

AUTHOR CONTRIBUTIONS

OGI contributed to study design, performed experiments, analyzed the data, performed statistical analysis, and wrote the paper; FB generated the mouse colony; MP performed experiments and contributed to data analysis; EP performed experiments and contributed to data analysis and to manuscript final editing; CP and MC performed histology; MA contributed to perform the experiments; PAC and AMR performed lipidomic analysis; MF, MB, RM, GM, PL, and BS provided human samples, metabolomics, and transcriptomics data; TS provided SOD2flox mice; CS provided medical expertise and double checked the clinical relevance of the data; GV contributed to the writing of the paper; AM designed the study, supervised the project, and wrote the paper. All authors discussed the results and commented on the manuscript.

DECLARATION OF INTERESTS

The authors declare no competing interests.

Received: January 20, 2021
Revised: October 19, 2021
Accepted: December 23, 2021
Published: January 21, 2022

REFERENCES

Alzoghaibi, M.A. (2013). Concepts of oxidative stress and antioxidant defense in Crohn's disease. World J. Gastroenterol. *19*, 6540–6547.

Balaban, R.S., Nemoto, S., and Finkel, T. (2005). Mitochondria, oxidants, and aging. Cell *120*, 483–495.

Band, A.M., Jones, P.M., and Howell, S.L. (1993). The mechanism of arachidonic acid-induced insulin secretion from rat islets of Langerhans. Biochim.Biophys. Acta *1176*, 64–68.

Bellafante, E., Morgano, A., Salvatore, L., Murzilli, S., Di, T.G., D'Orazio, A., Latorre, D., Villani, G., and Moschetta, A. (2014). PGC-1beta promotes enterocyte lifespan and tumorigenesis in the intestine. Proc. Natl. Acad. Sci. U S A. *111*, E4523–E4531.

Blaser, H., Dostert, C., Mak, T.W., and Brenner, D. (2016). TNF and ROS crosstalk in inflammation. Trends Cell Biol. *26*, 249–261.

Bresciani, G., da Cruz, I.B., and Gonzalez-Gallego, J. (2015). Manganese superoxide dismutase and oxidative stress modulation. Adv. Clin. Chem. *68*, 87–130.

Campbell, E.L., and Colgan, S.P. (2018). Control and dysregulation of redox signalling in the gastrointestinal tract. Nat. Rev. Gastroenterol. Hepatol. *16*, 106–120.

D'Errico, I., Salvatore, L., Murzilli, S., Lo, S.G., Latorre, D., Martelli, N., Egorova, A.V., Polishuck, R., Madeyski-Bengtson, K., Lelliott, C., et al. (2011). Peroxisome proliferator-activated receptor-gamma coactivator 1-alpha (PGC1alpha) is a metabolic regulator of intestinal epithelial cell fate. Proc. Natl. Acad. Sci. U S A. *108*, 6603–6608.

Ding, S., and Lund, P.K. (2011). Role of intestinal inflammation as an early event in obesity and insulin resistance. Curr.Opin.Clin.Nutr.Metab. Care *14*, 328–333.

Donahue, S.M., Rifas-Shiman, S.L., Gold, D.R., Jouni, Z.E., Gillman, M.W., and Oken, E. (2011). Prenatal fatty acid status and child adiposity at age 3 y: results from a US pregnancy cohort. Am. J. Clin.Nutr. *93*, 780–788.

Dowling, E.J., Chander, C.L., Claxson, A.W., Lillie, C., and Blake, D.R. (1993). Assessment of a human recombinant manganese superoxide dismutase in models of inflammation. Free Radic. Res. Commun. *18*, 291–298.

Ducheix, S., Peres, C., Hardfeldt, J., Frau, C., Mocciaro, G., Piccinin, E., Lobaccaro, J.M., De, S.S., Chieppa, M., Bertrand-Michel, J., et al. (2018). Deletion of stearoyl-CoA desaturase-1 from the intestinal epithelium promotes inflammation and tumorigenesis, reversed by dietary oleate. Gastroenterology *155*, 1524–1538.

Ellulu, M.S., Patimah, I., Khaza'ai, H., Rahmat, A., and Abed, Y. (2017). Obesity and inflammation: the linking mechanism and the complications. Arch. Med. Sci. *13*, 851–863.

Gaillard, D., Negrel, R., Lagarde, M., and Ailhaud, G. (1989). Requirement and role of arachidonic acid in the differentiation of pre-adipose cells. Biochem. J. *257*, 389–397.

Halliwell, B. (1993). The role of oxygen radicals in human disease, with particular reference to the vascular system. Haemostasis *23*, 118–126.

Han, Y.H., Buffolo, M., Pires, K.M., Pei, S., Scherer, P.E., and Boudina, S. (2016). Adipocyte-specific deletion of manganese superoxide dismutase Protects from diet-induced obesity through increased mitochondrial uncoupling and biogenesis. Diabetes *65*, 2639–2651.

Hayakawa, M., Ishida, N., Takeuchi, K., Shibamoto, S., Hori, T., Oku, N., Ito, F., and Tsujimoto, M. (1993). Arachidonic acid-selective cytosolic phospholipase A2 is crucial in the cytotoxic action of tumor necrosis factor. J. Biol. Chem. *268*, 11290–11295.

Heller, R.A., and Kronke, M. (1994). Tumor necrosis factor receptor-mediated signaling pathways. J.Cell Biol. *126*, 5–9.

Higdon, J.V., and Frei, B. (2003). Obesity and oxidative stress: a direct link to CVD? Arterioscler Thromb.Vasc. Biol. *23*, 365–367.

Hoeck, W.G., Ramesha, C.S., Chang, D.J., Fan, N., and Heller, R.A. (1993). Cytoplasmic phospholipase A2 activity and gene expression are stimulated by tumor necrosis factor: dexamethasone blocks the induced synthesis. Proc. Natl. Acad. Sci. U S A. *90*, 4475–4479.

Ikegami, T., Suzuki, Y., Shimizu, T., Isono, K., Koseki, H., and Shirasawa, T. (2002). Model mice for tissue-specific deletion of the manganese superoxide dismutase (MnSOD) gene. Biochem.Biophys. Res. Commun. *296*, 729–736.

James, M.J., Gibson, R.A., and Cleland, L.G. (2000). Dietary polyunsaturated fatty acids and inflammatory mediator production. Am. J. Clin.Nutr. *71*, 343S–348S.

Jenner, P. (1994). Oxidative damage in neurodegenerative disease. Lancet *344*, 796–798.

Jump, D.B., Clarke, S.D., Thelen, A., and Liimatta, M. (1994). Coordinate regulation of glycolytic and lipogenic gene expression by polyunsaturated fatty acids. J. Lipid Res. *35*, 1076–1084.

Kahn, B.B., and Flier, J.S. (2000). Obesity and insulin resistance. J. Clin.Invest. *106*, 473–481.

Kappel, B.A., De, A.L., Heiser, M., Ballanti, M., Stoehr, R., Goettsch, C., Mavilio, M., Artati, A., Paoluzi, O.A., Adamski, J., et al. (2020). Cross-omics analysis revealed gut microbiome-related metabolic pathways underlying atherosclerosis development after antibiotics treatment. Mol. Metab. *36*, 100976.

Keaney, J.F., Jr., Larson, M.G., Vasan, R.S., Wilson, P.W., Lipinska, I., Corey, D., Massaro, J.M., Sutherland, P., Vita, J.A., and Benjamin, E.J. (2003). Obesity and systemic oxidative stress: clinical correlates of oxidative stress in the Framingham Study. Arterioscler Thromb.Vasc. Biol. *23*, 434–439.

Kromhout, D., and de, G.J. (2014). Update on cardiometabolic health effects of omega-3 fatty acids. Curr.Opin.Lipidol. *25*, 85–90.

Li, C., and Zhou, H.M. (2011). The role of manganese superoxide dismutase in inflammation defense. Enzyme Res. *2011*, 387176.

Li, Y., Huang, T.T., Carlson, E.J., Melov, S., Ursell, P.C., Olson, J.L., Noble, L.J., Yoshimura, M.P., Berger, C., Chan, P.H., et al. (1995). Dilated cardiomyopathy and neonatal lethality in mutant mice lacking manganese superoxide dismutase. Nat. Genet. *11*, 376–381.

Lin, S.A., and Barker, N. (2011). Gastrointestinal stem cells in self-renewal and cancer. J. Gastroenterol. *46*, 1039–1055.

Madesh, M., and Balasubramanian, K.A. (1997). Activation of liver mitochondrial phospholipase A2 by superoxide. Arch. Biochem.Biophys. *346*, 187–192.

McMurray, F., Patten, D.A., and Harper, M.E. (2016). Reactive oxygen species and oxidative stress in obesity-recent findings and empirical approaches. Obesity (Silver Spring) *24*, 2301–2310.

Mittal, M., Siddiqui, M.R., Tran, K., Reddy, S.P., and Malik, A.B. (2014). Reactive oxygen species in inflammation and tissue injury. Antioxid. Redox Signal *20*, 1126–1167.

Miyamoto, J., Igarashi, M., Watanabe, K., Karaki, S.I., Mukouyama, H., Kishino, S., Li, X., Ichimura, A., Irie, J., Sugimoto, Y., et al. (2019). Gut microbiota confers host resistance to obesity by metabolizing dietary polyunsaturated fatty acids. Nat. Commun. *10*, 4007.

Montano, M.A., Barrio Lera, J.P., Gottlieb, M.G., Schwanke, C.H., da Rocha, M.I., Manica-Cattani, M.F., dos Santos, G.F., and da Cruz, I.B. (2009). Association between manganese superoxide

dismutase (MnSOD) gene polymorphism and elderly obesity. Mol.Cell Biochem. *328*, 33–40.

Murakami, M., and Kudo, I. (2002). Phospholipase A2. J. Biochem. *131*, 285–292.

Murphy, M.P. (2009). How mitochondria produce reactive oxygen species. Biochem. J. *417*, 1–13.

Naughton, S.S., Mathai, M.L., Hryciw, D.H., and McAinch, A.J. (2016). Linoleic acid and the pathogenesis of obesity. Prostaglandins Other Lipid Mediat. *125*, 90–99.

Nojiri, H., Shimizu, T., Funakoshi, M., Yamaguchi, O., Zhou, H., Kawakami, S., Ohta, Y., Sami, M., Tachibana, T., Ishikawa, H., et al. (2006). Oxidative stress causes heart failure with impaired mitochondrial respiration. J. Biol. Chem. *281*, 33789–33801.

Owen, J.L., Zhang, Y., Bae, S.H., Farooqi, M.S., Liang, G., Hammer, R.E., Goldstein, J.L., and Brown, M.S. (2012). Insulin stimulation of SREBP-1c processing in transgenic rat hepatocytes requires p70 S6-kinase. Proc. Natl. Acad. Sci. U S A. *109*, 16184–16189.

Persaud, S.J., Muller, D., Belin, V.D., Kitsou-Mylona, I., Asare-Anane, H., Papadimitriou, A., Burns, C.J., Huang, G.C., Amiel, S.A., and Jones, P.M. (2007). The role of arachidonic acid and its metabolites in insulin secretion from human islets of langerhans. Diabetes *56*, 197–203.

Pickens, C.A., Sordillo, L.M., Zhang, C., and Fenton, J.I. (2017). Obesity is positively associated with arachidonic acid-derived 5- and 11-hydroxyeicosatetraenoic acid (HETE). Metabolism *70*, 177–191.

Shimizu, T., Nojiri, H., Kawakami, S., Uchiyama, S., and Shirasawa, T. (2010). Model mice for tissue-specific deletion of the manganese superoxide dismutase gene. Geriatr.Gerontol. Int. *10*, S70–S79.

Sies, H., and Jones, D.P. (2020). Reactive oxygen species (ROS) as pleiotropic physiological signalling agents. Nat. Rev. Mol.CellBiol. *21*, 363–383.

Simopoulos, A.P. (2016). An increase in the omega-6/omega-3 fatty acid ratio increases the risk for obesity. Nutrients *8*, 128.

Spagnuolo, M.I., Cicalese, M.P., Caiazzo, M.A., Franzese, A., Squeglia, V., Assante, L.R., Valerio, G., Merone, R., and Guarino, A. (2010). Relationship between severe obesity and gut inflammation in children: what's next? Ital. J. Pediatr. *36*, 66.

Tan, H.Y., Wang, N., Li, S., Hong, M., Wang, X., and Feng, Y. (2016). The reactive oxygen species in macrophage polarization: reflecting its dual role in Progression and treatment of human diseases. Oxid.Med.Cell Longev. *2016*, 2795090.

Ungaro, F., Tacconi, C., Massimino, L., Corsetto, P.A., Correale, C., Fonteyne, P., Piontini, A., Garzarelli, V., Calcaterra, F., Della, B.S., et al. (2017). MFSD2A promotes endothelial generation of inflammation-resolving lipid mediators and reduces ColitisÂ inÂ mice. Gastroenterology *153*, 1363–1377.

Wang, L., Manson, J.E., Rautiainen, S., Gaziano, J.M., Buring, J.E., Tsai, M.Y., and Sesso, H.D. (2016). A prospective study of erythrocyte polyunsaturated fatty acid, weight gain, and risk of becoming overweight or obese in middle-aged and older women. Eur. J. Nutr. *55*, 687–697.

Zelko, I.N., Mariani, T.J., and Folz, R.J. (2002). Superoxide dismutase multigene family: a comparison of the CuZn-SOD (SOD1), Mn-SOD (SOD2), and EC-SOD (SOD3) gene structures, evolution, and expression. Free Radic. Biol. Med. *33*, 337–349.

STAR★METHODS

KEY RESOURCES TABLE

REAGENT or RESOURCE	SOURCE	IDENTIFIER
Antibodies		
Recombinant anti-Insulin	Abcam	Cat# ab181547; RRID:AB_2716761
Rabbit polyclonal anti-Nitrotyrosine	Abcam	Cat# ab42789; RRID:AB_776782
Dako REAL EnVision Detection System, Peroxidase/DAB, Rabbit/Mouse, HRP Kit	Agilent	Cat# K5007; RRID:AB_2888627
Biological samples		
Human colon samples	FLOROMIDIA cohort (Kappel et al. 2020)	N/A
Critical commercial assays		
Cholesterol Liquid	Sentinel	Cat# 17644H
Triglycerides Liquid	Sentinel	Cat# 17624H
Phospholipids	Sentinel	Cat# 17320
Rat/mouse Insulin ELISA	Merck	Cat# EZRMI-13K
Mouse LBP ELISA	Abcam	Cat# ab213876
Multi Species GLP-1 Total ELISA	Sigma-Aldrich	Cat# EZGLP1T-36K
Lipid peroxidation (MDA) assay	Abcam	Cat# ab118970
$cPLA_2$ assay	Cayman Chemical	Cat# 765021
Deposited data		
FLOROMIDIA database	Kappel et al. 2020	GEO: GSE158237
Experimental models: Organisms/strains		
Intestinal-specific *Sod2* deficient mice	Generated in this study	N/A
Sod2 flox/flox mice	Ikegami et al. 2002	N/A
Vill-Cre mice	Jackson Laboratory	Cat# 004586
Oligonucleotides		
Primers for qPCR, see Table S1	This study	N/A
Software and algorithms		
Aperio Imagescope software 12.3.3	Leica Biosystems	https://www.leicabiosystems.com/digital-pathology/manage/aperio-imagescope/
GraphPad Prism version 6.01 and 8.01	GraphPad Software	https://www.graphpad.com/scientific-software/prism/
Other		
Essential fatty acid deficient diet	Research Diet	Cat# D15013004

RESOURCE AVAILABILITY

Lead contact

Further information and requests for resources and reagents should be directed to and will be fulfilled by the lead contact, Antonio Moschetta (antonio.moschetta@uniba.it).

Materials availability

All materials generated in this study are available through reasonable request to the lead contact Antonio Moschetta (antonio.moschetta@uniba.it).

Data and code availability

- This paper analyzes existing, publicly available data. These accession numbers for the datasets are listed in the key resources table.
- This paper does not report original code.
- Any additional information required to reanalyze the data reported in this paper is available from the lead contact upon request.

EXPERIMENTAL MODEL AND SUBJECT DETAILS

Generation of mouse models and experimental settings

Intestine-specific SOD2 deletion (iSOD2KO) was obtained by crossing SOD2flox/flox (SOD2flox) mice (obtained from Dr. Takuji Shirasawa of the Tokyo Metropolitan Institute of Gerontology) (Ikegami et al., 2002), in which the third exon of the *Sod2* gene was flanked by loxp sequences, with Vil1in-Cre (vill-Cre) transgenic mice (Jackson Laboratory). The resulting heterozygous SOD2flox and vill-Cre transgenic mice were mated with homozygous SOD2flox mice in order to generate the iSOD2KO mice. Homozygous male iSOD2KO mice and their corresponding control SOD2flox littermates were used throughout this study. All murine strains used were on a C57BL/6 background. At least 8 mice were used per condition. Mice were sacrificed at the indicated time points (6–8 months of age). Mice were fed chow or essential fatty acid deficient (EFAD) diet (D15013004 from Research Diet, New Brunswick, USA) for 3 months starting at 3 months of age. The composition of the diets has been described before (Ducheix et al., 2018). All mice were housed in a pathogen-free facility, in a temperature-controlled room (21 $\pm$ 2°C) on a 12-hour light/dark cycle and with *ad libitum* access to food and water. Body weight and food intake were measured weekly. For food intake experiment, we followed a standard protocol. Briefly, the amount of food (in grams) added to the single mouse cage was recorded before administration. After a week, we measured the food left on the cage and we calculated the food consumed (Total food - food left = Food consumed). Plasma was collected and intestine, epididymal white adipose tissue (WAT), liver, and pancreas tissue samples were either snap-frozen in liquid nitrogen or formalin fixed and paraffin embedded for subsequent histological analysis. The Ethical Committee of the University of Bari approved this experimental setup, also certified by the Italian Ministry of Health in accordance with internationally accepted guidelines for animal care.

Human samples

The FLOROMIDIA database was already described (Kappel et al., 2020). All subjects gave written informed consent, validated and approved by the ethical committee of Policlinico Tor Vergata University of Rome (Comitato Etico Indipendente, approval number 28-05-2009). The human subject cohort comprised 42 subjects (58,48 years of age $\pm$9,235) recruited at the Department of Medicine Policlinico Tor Vergata. Sample size was not determined by statistical methods, given the exploratory nature of the project. Colon transcriptomics was performed with Affymetrix HUGENE 2.0 ST ARRAY FORMAT 100 (GEO Accession Number: GSE158237); SOD2 expression levels normalized with RMA method were used in this study. Analysis of arachidonic acid metabolites was performed in service by Metabolon inc. (USA) and previously described (Kappel et al., 2020). Integrated metabolomics and transcriptomics analysis of the complete FLOROMIDIA database will be described in another manuscript.

METHOD DETAILS

RNA extraction and real time qPCR

Total RNA was extracted using QIAzol reagent (Qiagen, Hilden, Germany) and the Qiagen TissueLyser (Qiagen) following the manufacture's instruction. Total RNA samples (2 μg) were treated with DNase (Thermo Fisher Scientific, Waltham, Massachusetts, USA) and reverse-transcribed using High Capacity cDNA Reverse Transcription Kit (Thermo Fisher Scientific). Real-time quantitative PCR was performed with Power SYBR Green (Thermo Fisher Scientific) in an Applied Biosystems QuantStudio5 machine (Thermo Fisher Scientific). Gene expression was determined using the ΔΔCT calculation normalizing by the TATA-box binding protein (Tbp) mRNA levels. The sequence of the primers used to detect mRNA expression levels for the genes investigated in this study are available in the Table S1.

Histological and immunohistochemical studies

Ileum, liver, and pancreas tissue samples were fixed in formalin during 24 h, dehydrated and paraffin embedded. WAT samples, stored at −80°C, were directly dehydrated and paraffin embedded. Paraffin-embedded sections were cut at 4μm thick and were stained with hematoxylin-eosin following standard protocols. For immuno-histochemical analysis, paraffin-embedded organ sections were subjected to antigen retrieval by boiling the slides in sodium citrate pH 6 (Sigma Aldrich) for 15min. Sections were washed 3 times with 1% PBS, sequentially incubated in protein blocking solution (room temperature, 10min; Dako, Glostrup, Denmark) and incubated with the primary anti-Insulin antibody (EPR17359, ab181547, Abcam, Cambridge, UK) at 1:60.000 dilution (room temperature) or primary anti-Nitrotyrosine antibody (ab42789, Abcam, Cambridge, UK) at 1:100 dilution (+4°C). After washes, sections were then incubated with anti-rabbit HRP-linked secondary antibody revelation system (K5007, Dako/Agilent). Sections were counterstained with hematoxylin, mounted with Gel mount (C0563, Dako) and observed under light microscope. Light microscopy micrographs were captured by Coolpix 990 digital camera (Nikon, Calenzano, Italy) connected to a Leica Leitz DMRBE microscope (Leica Biosystems, Nussloch, Germany). Morphometric measurements of the insulin-immunostained sections were performed using the Aperio Imagescope software (Leica Biosystems). The average area of the Langerhans islets was determined by measuring the insulin-inmunostained area in 6 different X10 microscopic fields from 5 mice from each group.

Plasma analysis

Blood samples were collected by cardiac puncture in lithium-heparin collection tubes at the time of the sacrifice. Plasma was prepared by low speed centrifugation at 4°C. Aliquots were immediately frozen and stored at −80°C until assayed. Plasma levels of cholesterol, triglycerides and phospholipids were measured using colorimetric kits (Sentinel Diagnostic, Milan, Italy) according to manufacturer's instructions. Plasma levels of insulin were measured by a rat/mouse insulin ELISA kit (EZRMI-13K, Merck Millipore, Darmstadt, Germany) following the manufacturer's instructions. Lipopolysaccharides Binding Protein levels in plasma were measured by Mouse LBP ELISA Kit (ab213876, Abcam, Cambridge, UK). GLP1 plasma levels were assayed with Multi Species GLP-1 Total ELISA (Merck-Millipore, Burlington, Massachusetts, USA). Manufacturer's instructions were followed.

Oral glucose tolerance test

Oral glucose tolerance test was performed following an overnight fast. Mice were oral gavaged with 2g D-glucose/kg body weight. Blood glucose, obtained 30 minutes prior to glucose administration and at 0, 15, 30, 60 and 120 minutes post-gavage from the tail vein, was quantified with an OG Care glucometer (Biochemical Biosystems International, Arezzo, Italy). Area under the curve (AUC) was calculated using GraphPad Prism (GraphPad Software, San Diego, USA)

HOMA-IR

The Homeostatic Model Assessment for Insulin Resistance (HOMA-IR) index was calculated as [(fasting glucose mmol/L x fasting insulin mU/L)/22,5)] to assess insulin resistance.

Lipid peroxidation

Lipid peroxidation (MDA) assay kit (ab118970, Abcam) was used to measure the levels of malondialdehyde (MDA), an end product of lipid peroxidation, in intestinal mucosal samples. Manufacturer's instructions were followed.

PLA2 activity

Phospholipase A2 (PLA2) activity was measured in intestinal mucosal samples using a colorimetric cytosolic PLA2 (cPLA2) assay kit (765021, Cayman Chemical, Ann Arbor, USA) following the manufacturer's instructions.

Lipid extraction

Plasma and tissue lipids were extracted according to Folch with minor modifications as previously described (Ungaro et al., 2017). Briefly, samples were homogenized with chloroform/methanol 1:2, centrifuged to recover the lipid extract and extracted again two times. Plasma was lyophilized before extraction. Each solvent used for extraction and analysis contained 0.045 mM 3,5-di-tert-4-butylhydroxytoluene (BHT) to avoid PUFA oxidation.

Free fatty acid analysis

Free fatty acid composition of samples was determined by gas chromatography (Thermo-Fischer TRACE 1300/1310) equipped with a flame ionization detector (FID) under the following experimental conditions: column: Nukol, 15 m × 0.53 mm I.D., 0.5 μm (Sigma, Aldrich); oven 110°C, 8°C/min to 220°C; carrier gas helium, 20 mL/min; inj. temperature 250°C and detector FID temperature, 250°C. Prior to lipid extraction, a known amount of internal standard (C17:0) was added to each sample to correct for yield and recovery. A standard mixture containing all free fatty acid was daily injected as calibration for quantitative analysis.

QUANTIFICATION AND STATISTICAL ANALYSIS

Data are expressed as means ± SEM. Analyses were performed using GraphPad Prism version 6.01 and 8.01 (GraphPad Software, San Diego, USA). Data were compared between pairs of groups using the Student *t*-test and correlation analysis in human data was performed by Spearman's correlation. A *p* value of <0,05 was considered significant.